CHAPTER 28

On the Joint Distribution of Wave Height, Period and Direction of Individual Waves in a Three-Dimensional Random Seas

J.G.Kwon[1] and Ichiro Deguchi[2]

Abstract

A theoretical expression for the joint disribution of wave height, period and direction is derived based on the hypothesis that sea surface is a Gaussian stochastic process and that a band-width of energy spectra is sufficiently narrow. The derived joint distribution is found to be an effective measure to investigate characteristics of three-dimensional random wave fields in shallow water through field measurements.

I. Introduction

A variety of studies has been conducted on the sediment transport in shallow water regions and a lot of formula has been proposed on the rate of sediment transport. However, these formulas do not always predict the same estimation of the rate of sediment transport even under the same conditions. This discrepancy can be explained by the following reasons: i) the dynamics and kinematics of sediment movement are not fully understood yet and each formula contains empirical coefficients which have to be fixed through experiments or field measurements, and ii) the accurate measurement of sediment transport rate is extremely difficult. In the case of applying these formula to the sediment transport in the fields, further difficulties such as how to take into account the effect of irregularities in wave heights, periods and directional spreading of incident waves arise.

On the other hand, a wave transformation including wave breaking in the shallow water reigion is a

[1] Assistant Professor, Dept. of Environmental Eng., Pusan Univ., Changjun-dong, Kumjeoung-ku, Pusan, 609-735, Korea

[2] Assistant Professor, Dept. of Civil Eng., Osaka Univ., 2-1 Yamadaoka, Suita City, Osaka 565, Japan

non-linear and discontinuous phenomenon. Therefore, a so-called individual wave analysis (or a wave-by-wave analysis) rather than spectral approach seems to be adequate to investigate the wave transforation in such regions.

In this study, a joint distribution of wave height, period and direction of zero-down crossing waves which is required in the individual wave analysis in the shallow water region is derived theoretically. The applicability of the derived joint distribution, which is hereafter referred to as H-T-θ joint distribution, to the shallow water waves in the fields is examined through fields observations.

II. Derivation of H-T-θ Joint Distribution

2.1 Expression of Waves in Three-dimensional Random Seas

In a deep water region where a dispersive property of wave is strong, three-dimensional random seas waves are expressed by a directional spectrum. A transformation of irregular waves is also analyzed as the transformation of directional spectrum. While wave transformations in the shallow water region, where a significant sediment transport takes place, are usually investigated by applying the individual wave analysis (or the wave-by-wave analysis) of zero-down(or up)-crossing waves due to the non-linearity and discontinuity caused by wave breaking. The applicability of this approach has already been verified through experiments in two-dimensional wave tanks (for example, Mase et al., 1982).

The authors aim at applying the individual wave analysis to the three-dimensional random sea waves in shallow water with directional spreading. To do so, the joint distribution of wave height, period and direction of individual zero-down(or up)crossing waves has to be given.

Theoretical investigations on the joint probability density functions of H-T and H-θ have been conducting assuming that the band width of the frequency spectra of surface displacement $\eta(t)$ is sufficiently narrow so that $\eta(t)$ can be expressed by the envelope function. In this paper, referring to these results, the joint distribution of H-T-θ is derived from envelpe functions of surface displacements $\eta(t)$, bi-directional water particle velocities u(t), v(t) and time derivatives of surface displacements $\dot{\eta}(t)$.

The surface displacement in three-dimensional random sea is usually expressed by the sum of an infinite number of sine-waves of amplitudes a_{ij} and periods T_i , each of which has different wave direction θ_j , in the following form :

$$\eta(t) = \sum_{i=1}^{\infty}\sum_{j=1}^{\infty} a_{ij}\cos\phi_{ij} \tag{1}$$

$$\phi_{ij} = k_i(x\cos\theta_j + y\sin\theta_j) - 2\pi f_i t - \varepsilon_{ij} \tag{2}$$

where k_i are the wave numbers and f_i are the frequencies, both of which correspond to the periods T_i , θ_j are the wave directions and ε_{ij} represent the phase differences of the waves whose amplitudes are a_{ij} . A coordinate system used in this study is shown in Fig.1 .

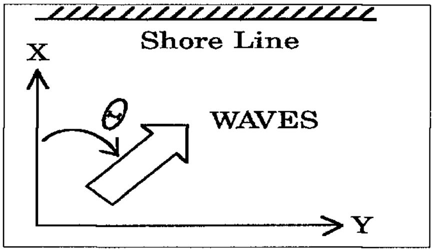

Fig. 1 Coordinate system

In the same way, water particle velocities in x- and y-directions u(t), v(t) are expressed as follows :

$$u(t) = \sum_{i=1}^{\infty}\sum_{j=1}^{\infty} b_i\cos\theta_j\, a_{ij}\cos\phi_{ij} \tag{3}$$

$$v(t) = \sum_{i=1}^{\infty}\sum_{j=1}^{\infty} b_i\sin\theta_j\, a_{ij}\cos\phi_{ij} \tag{4}$$

$$b_i = 2\pi f_i\,\frac{\cosh k_i z}{\sinh k_i h} \tag{5}$$

where, z is the height from the bottom where water particle velocities were measured..

Besides these three time series, a time derivative of the surface elevation $\dot{\eta}(t)$ which is expressed by Eq.(6) is required to obtain the H-T-θ joint distribution.

$$\dot{\eta}(t) = \sum_{i=1}^{\infty}\sum_{j=1}^{\infty} 2\pi f_i a_{ij} \sin\phi_{ij} \tag{6}$$

2.2 Envelope Functions

To express envelopes of time series of the quantities given by Eqs.(1), (3), (4) and (6), the phase function given by Eq.(2) is rewritten by using a representative frequency $\bar{f}$ as,

$$\phi_{ij}^{\cdot} = k_i(x\cos\theta_j + y\sin\theta_j) - 2\pi(f_i - \bar{f})t - \varepsilon_{ij} \tag{7}$$

Substituting Eq.(7) into Eqs.(1) , (3), (4) and (6), the following envelope functions of time series of $\eta(t)$, u(t), v(t) and $\dot{\eta}(t)$ are obtained :

$$\begin{aligned}
\eta(t) &= \eta_c(t)\cos 2\pi\bar{f}t + \eta_s(t)\sin 2\pi\bar{f}t \\
\dot{\eta}(t) &= \dot{\eta}_c(t)\cos 2\pi\bar{f}t + \dot{\eta}_s(t)\sin 2\pi\bar{f}t \\
u(t) &= u_c(t)\cos 2\pi\bar{f}t + u_s(t)\sin 2\pi\bar{f}t \\
v(t) &= v_c(t)\cos 2\pi\bar{f}t + v_s(t)\sin 2\pi\bar{f}t
\end{aligned} \tag{8}$$

where,

$$\begin{aligned}
\eta_c(t) &= \sum_{i=1}^{\infty}\sum_{j=1}^{\infty} a_{ij}\cos\phi_{ij}^{\cdot} \\
\eta_s(t) &= \sum_{i=1}^{\infty}\sum_{j=1}^{\infty} a_{ij}\sin\phi_{ij}^{\cdot} \\
\dot{\eta}_c(t) &= \sum_{i=1}^{\infty}\sum_{j=1}^{\infty} 2\pi(f_i - \bar{f})\, a_{ij}\sin\phi_{ij}^{\cdot} \\
\dot{\eta}_s(t) &= \sum_{i=1}^{\infty}\sum_{j=1}^{\infty} 2\pi(f_i - \bar{f})\, a_{ij}\cos\phi_{ij}^{\cdot} \\
u_c(t) &= \sum_{i=1}^{\infty}\sum_{j=1}^{\infty} b_i\cos\theta_j\, a_{ij}\cos\phi_{ij}^{\cdot} \\
u_c(t) &= \sum_{i=1}^{\infty}\sum_{j=1}^{\infty} b_i\cos\theta_j\, a_{ij}\cos\phi_{ij}^{\cdot} \\
u_s(t) &= \sum_{i=1}^{\infty}\sum_{j=1}^{\infty} b_i\cos\theta_j\, a_{ij}\sin\phi_{ij}^{\cdot} \\
v_c(t) &= \sum_{i=1}^{\infty}\sum_{j=1}^{\infty} b_i\sin\theta_j\, a_{ij}\cos\phi_{ij}^{\cdot} \\
v_s(t) &= \sum_{i=1}^{\infty}\sum_{j=1}^{\infty} b_i\sin\theta_j\, a_{ij}\sin\phi_{ij}^{\cdot}
\end{aligned} \tag{9}$$

The amplitude of each carrier wave and the phase relation between carrier waves and water particle velocities are determined by these envelope functions.

2.3 Joint Probability Density Function of Envelope Amplitudes

As can be understood from Eq.(8), these eight envelope amplitudes are stationary Gaussian stochastic processes with zero mean by virtue of the central limit theorem. Therefore, the probability density function for eight envelope amplitudes is expressed as :

$$
\begin{aligned}
&P\,(\eta_c, \eta_s, u_c, u_s, v_c, v_s, \dot{\eta}_c, \dot{\eta}_s) \\
&= \frac{1}{(2\pi)^4\,[M]^{1/2}}\,\mathrm{EXP}\,\left[-\frac{1}{2}\sum_{i=1}^{8}\sum_{j=1}^{8}\frac{M_{ij}}{[M]}\,\zeta_i\zeta_j\right] \\
&= \frac{1}{(2\pi)^4(m_{00}\,m_{02}\,m_{20}\,m_{22})} * \mathrm{EXP}\,\left[-\frac{1}{2*\Delta} * \left\{A_{11}\left(\frac{\dot{\eta}_c^{\,2}+\dot{\eta}_s^{\,2}}{m_{00}}\right)\right.\right. \\
&\quad + A_{22}\left(\frac{u_c^2+u_s^2}{m_{20}}\right) + A_{44}\left(\frac{\eta_c^2+\eta_s^2}{m_{22}}\right) + A_{33}\left(\frac{v_c^2+v_s^2}{m_{02}}\right) + \\
&\quad 2A_{12}\left(\frac{\eta_c u_c+\eta_s u_s}{\sqrt{m_{00}\,m_{20}}}\right) + 2A_{13}\left(\frac{\eta_c v_c+\eta_s v_s}{\sqrt{m_{00}\,m_{02}}}\right) + 2A_{23}\left(\frac{u_c v_c+u_s v_s}{\sqrt{m_{02}\,m_{20}}}\right) + \\
&\quad 2A_{14}\left(\frac{\eta_c\dot{\eta}_s+\dot{\eta}_c\eta_s}{\sqrt{m_{00}\,m_{22}}}\right) + 2A_{24}\left(\frac{u_c\dot{\eta}_s-u_s\dot{\eta}_c}{\sqrt{m_{22}\,m_{20}}}\right) + 2A_{34}\left(\frac{v_c\dot{\eta}_s-v_s\dot{\eta}_c}{\sqrt{m_{22}m_{02}}}\right)\Big]
\end{aligned}
\tag{10}
$$

where,

$$
[M] = \begin{pmatrix} M_0 & 0 \\ & \\ 0 & M_0' \end{pmatrix}, \qquad M_0 = \begin{pmatrix} m_{00} & m_{10} & m_{01} & 0 \\ m_{10} & m_{20} & m_{11} & m_{12} \\ m_{01} & m_{11} & m_{02} & m_{21} \\ 0 & m_{12} & m_{21} & m_{22} \end{pmatrix},
$$

$$
M_0' = \begin{pmatrix} m_{00} & m_{10} & m_{01} & 0 \\ m_{10} & m_{20} & m_{11} & -m_{12} \\ m_{01} & m_{11} & m_{02} & -m_{21} \\ 0 & -m_{12} & -m_{21} & m_{22} \end{pmatrix}
$$

is the determinant of covariance matrix whose elements $<\zeta_i, \zeta_j>$ are defined as :

$$
\begin{aligned}
&\langle \eta_c\eta_c \rangle = \langle \eta_s\eta_s \rangle = \langle \eta^2 \rangle = m_{00}\,, \quad \langle \eta_c v_c \rangle = \langle \eta_s v_s \rangle = \langle \eta v \rangle = m_{01} \\
&\langle u_c u_c \rangle = \langle u_s u_s \rangle = \langle u^2 \rangle = m_{20}\,, \quad \langle u_c v_c \rangle = \langle u_s v_s \rangle = \langle uv \rangle = m_{11}
\end{aligned}
\tag{11}
$$

$$\langle v_c v_c \rangle = \langle v_s v_s \rangle = \langle v^2 \rangle = m_{02} , \ \langle \dot{\eta}_c \dot{\eta}_c \rangle = \langle \dot{\eta}_s \dot{\eta}_s \rangle = \langle \dot{\eta}^2 \rangle = m_{22}$$
$$\langle \eta_c u_c \rangle = \langle \eta_s u_s \rangle = \langle \eta u \rangle = m_{10} , \ \langle u_c \dot{\eta}_s \rangle = -\langle u_s \dot{\eta}_c \rangle = m_{12}$$
$$\langle v_c \dot{\eta}_s \rangle = -\langle v_s \dot{\eta}_c \rangle = m_{21} \qquad (11)$$

M_{ij} is the co-factor of $< \zeta_i , \zeta_j >$ and

$$\begin{aligned}
\Delta &= (1 + 2\gamma_{11}\gamma_{12}\gamma_{21} - \gamma_{12}^2 - \gamma_{21}^2 - \gamma_{11}^2 - \gamma_{10}^2 - 2\gamma_{01}\gamma_{10}\gamma_{12}\gamma_{21} \\
&\quad + 2\gamma_{10}\gamma_{01}\gamma_{11} + \gamma_{10}^2\gamma_{21}^2 + \gamma_{01}^2\gamma_{12}^2 - \gamma_{01}^2) \\
A_{11} &= (1 + 2\gamma_{11}\gamma_{12}\gamma_{21} - \gamma_{12}^2 - \gamma_{21}^2 - \gamma_{11}^2) \\
A_{12} &= (\gamma_{21}^2\gamma_{10} + \gamma_{01}\gamma_{11} - \gamma_{10} - \gamma_{01}\gamma_{12}\gamma_{21}) \\
A_{13} &= (\gamma_{10}\gamma_{11} + \gamma_{12}^2\gamma_{01} - \gamma_{10}\gamma_{12}\gamma_{21} - \gamma_{01}) \\
A_{14} &= (\gamma_{10}\gamma_{12} + \gamma_{01}\gamma_{21} - \gamma_{10}\gamma_{11}\gamma_{21} - \gamma_{01}\gamma_{11}\gamma_{12}) \\
A_{22} &= (1 - \gamma_{21}^2 - \gamma_{01}^2) \\
A_{23} &= (\gamma_{01}\gamma_{10} + \gamma_{12}\gamma_{21} - \gamma_{11}) \\
A_{24} &= (\gamma_{11}\gamma_{21} + \gamma_{01}^2\gamma_{12} - \gamma_{12} - \gamma_{10}\gamma_{01}\gamma_{21}) \\
A_{33} &= (1 - \gamma_{12}^2 - \gamma_{10}^2) \\
A_{44} &= (1 + 2\gamma_{10}\gamma_{01}\gamma_{11} - \gamma_{01}^2 - \gamma_{11}^2 - \gamma_{10}^2)
\end{aligned}$$

where,

$$\gamma_{10} = m_{10}/\sqrt{m_{00}\, m_{20}} , \ \gamma_{01} = m_{01}/\sqrt{m_{00}\, m_{02}} , \ \gamma_{11} = m_{11}/\sqrt{m_{20}\, m_{02}}$$
$$\gamma_{12} = m_{12}/\sqrt{m_{20}\, m_{22}} , \ \gamma_{21} = m_{21}/\sqrt{m_{02}\, m_{22}} , \qquad (12)$$

Among these nine covariances from m_{00} to m_{21} of preceding description, seven covariance except for m_{12} and m_{21} can be directly calculated from the time series of surface elevation η(t) and horizontal water particle velocities u(t) and v(t). While, m_{12} and m_{21} can be calculated from the directional spectra $s(f, \theta)$ as :

$$\begin{aligned}
m_{12} &= - \int_0^\infty \int_{-\pi}^{\pi} 2\pi b(f)(f - \bar{f}) \cos\theta \ \ s(f, \theta)\, d\theta df \\
m_{21} &= - \int_0^\infty \int_{-\pi}^{\pi} 2\pi b(f)(f - \bar{f}) \sin\theta \ \ s(f, \theta)\, d\theta df
\end{aligned} \qquad (13)$$

2.4 Joint Probability Density Function of Wave Height , Period and Direction

To derive the joint probability density function for wave height, period and direction, the following series of variable transformation are carried out :

1) Normalization of the envelope functions.

$$N_c = \eta_c/\sqrt{m_{00}}\,,\ N_s = \eta_s/\sqrt{m_{00}}\,,\ V_c = v_c/\sqrt{m_{02}}\,,\ V_s = v_s/\sqrt{m_{02}}\,,$$
$$U_c = u_c/\sqrt{m_{20}}\,,\ U_s = u_s/\sqrt{m_{20}}\,,\ \dot{N}_c = \dot{\eta}_c/\sqrt{m_{22}}\,,\ \dot{N}_s = \dot{\eta}_s/\sqrt{m_{22}}\,, \tag{14}$$

2) Introduction of the amplitude R and phase angle δ of carrier waves.

$$N_c = R\cos\delta \quad ,\quad N_s = R\sin\delta$$
$$\dot{N}_c = \dot{R}\cos\delta - R\,\dot{\delta}\sin\delta \ ,\quad \dot{N}_s = \dot{R}\sin\delta + R\,\dot{\delta}\cos\delta \tag{15}$$

where, $R^2 = N_c^2 + N_s^2$. $\delta = \tan^{-1}(N_s/N_c)$ (16)

3) Transformation of the phase angle of water particle velocities so that the phase of the surface displacement becomes a standard and introduction of the polar coordinate system after defining the wave direction of each wave θ(after Isobe, 1987).

$$U_c = u_p\cos\delta - u_q\sin\delta \quad ,\quad U_s = u_p\sin\delta + u_q\cos\delta$$
$$V_c = v_p\cos\delta - v_q\sin\delta \quad ,\quad V_s = v_p\sin\delta + v_q\cos\delta \tag{17}$$

$$\theta = \tan^{-1}(v_p/u_p)$$
$$u_p = W\cos\theta \quad ,\quad v_p = W/\Gamma\,\sin\theta \tag{18}$$

After conducting these transformation of variables of Eq.(10), the following joint probability density function for R , $\dot{\delta}$ and θ is obtained by integrating with respect to u_q , v_q , $\dot{R}$, δ and W which have nothing to do with H-T-θ joint distribution :

$$P(R,\theta,\dot{\delta}) = \frac{1}{2\pi^{3/2}*\Gamma} * R^2 * \mathrm{EXP}\left[\frac{R^2}{2\Delta}*(A_{11}+A_{44}\,\dot{\delta}^2+2A_{14}\dot{\sigma})\right] * \left[\frac{\sqrt{\Delta}}{A} + \frac{RB}{A^{3/2}}*\frac{\sqrt{\pi}}{\sqrt{2}}*\mathrm{EXP}\left\{\frac{R^2B^2}{2A\Delta}\right\}*\left\{1-\Pr\left(-\frac{RB}{\sqrt{A\Delta}}\right)\right\}\right] \tag{19}$$

where, $\Gamma = \sqrt{m_{02}/m_{20}}$ is a longcrestedness parameter and

$$\Pr(\zeta) = \frac{1}{\sqrt{2\pi}} * \int_{-\infty}^{\zeta} \exp\left(-\frac{t^2}{2}\right) dt$$
$$A = \left(A_{22} \cos\theta^2 + A_{33} \sin\theta^2 / \Gamma^2 + 2A_{23} \cos\theta \sin\theta / \Gamma\right)$$
$$B = -\left(A_{12} \cos\theta + A_{13} \sin\theta / \Gamma + A_{24} \dot{\delta} \cos\theta + A_{34} \dot{\delta} \sin\theta / \Gamma\right)$$

When the spectral bandwidth is sufficiently narrow, R and $\dot{\delta}$ in Eq.(19) can be related to the wave height $\overline{H}$ and the period $\overline{T}$ (Longuet - Higgins, 1975) as :

$$R = H/2\ , \quad \dot{\delta} = 2\pi(\bar{f} - f) = 2\pi(1/\overline{T} - 1/T) \tag{20}$$

By using these relations together with the zero-th and first special moments m_0 and m_1 , wave heights and periods are normalized as follows :

$$\begin{aligned} \tau &= T/\overline{T} = 2\pi/(2\pi\bar{f} - \dot{\delta}) * m_1/m_0 \\ x &= H/\overline{H} = 2R/(2\pi m_0)^{1/2} \end{aligned} \tag{21}$$

Substituting, Eq.(21) into Eq.(19), the following joint probability density function for wave heights(x), period (τ) and direction (θ) is obtained :

$$\begin{aligned} P(x, \tau, \theta) = {} & \frac{x^2 * \bar{\sigma}}{2^3 * \Gamma * \tau^2} * \mathrm{EXP}\left[-\frac{\pi}{4\Delta} * x^2 (A_{11} + A_{44} \bar{\sigma}^2 (1 - 1/\tau)^2\right. \\ & \left. + 2A_{14} \bar{\sigma} (1 - 1/\tau))\right] * \left[\frac{\sqrt{\Delta}}{A} + \frac{B'}{A^{3/2}} * \frac{\sqrt{\pi}}{\sqrt{2}} * x * \frac{\sqrt{\pi}}{\sqrt{2}}\right. \\ & \left. \mathrm{EXP}\left\{\frac{B'^2 \pi}{4A\Delta} x^2\right\} * \left\{1 - \Pr\left(-B' \frac{\sqrt{\pi}}{\sqrt{2A\Delta}} x\right)\right\}\right] \end{aligned} \tag{22}$$

where, $\bar{\sigma} = 2\pi m_1 m_0$ and

$$\begin{aligned} B' = {} & -\{A_{12} \cos\theta + A_{13} \sin\theta / \Gamma + A_{24} \bar{\sigma} (1 - 1/\tau) \cos\theta \\ & + A_{34} \bar{\sigma} (1 - 1/\tau) \sin\theta / \Gamma) \end{aligned}$$

Akai et al.(1988) also derived the joint distribution of wave height, frequency and direction. They omitted cross correlation term(γ_{21}) for influence of the asymmetrical property of directional spreading, but in our derivation, all correlation are taken into account.

III. H-T-θ Joint Distribution of Measured Waves in Shallow Water

3.1 Field Observation

Field observation were carried out at two coasts to verify the proposed joint probability density function for wave height, period and direction under the condition of wind waves in a winter. One observation site was the Keinomatsubara Beach located in the west coast of the Awaji Island and the other was the Nishikinohama Beach on the southern part of OSAKA Bay. These locations are shown in Fig. 2.

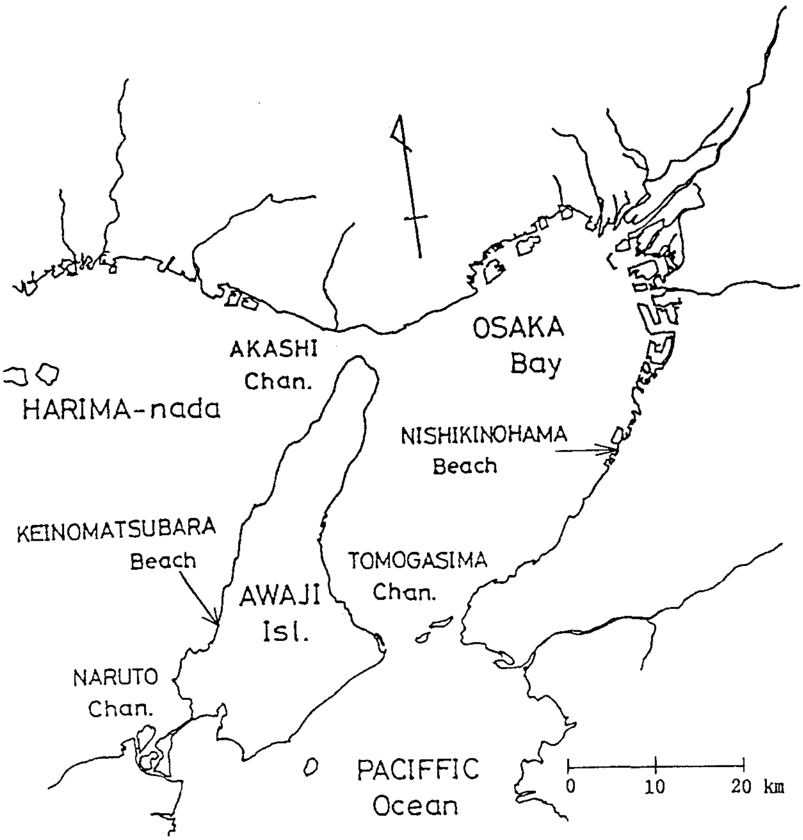

Fig. 2 Location of observation sites

Wave heights were measured by capacipitance type wave gages. Longshore and cross-shore water particle velocities were measured by bi-directional electromagnetic current meters at the same place of wave gauges and about 25cm above the bottom to consist a so-caled 3-element array. Analogue data from these installments were first recorded by an analogue data recorder and then digitized by an A-D converter at a sampling time of 0.1sec for the data processing. Very small waves whose frequencies were greater than $4*f_p$ (f_p : peak frequency) were disregarded in the data processing.

3.2 Characteristics of Measured Waves

Before discuss the joint distribution, characteristics of measured waves are examined briefly. Table 1 shows the statistical characteristics obtained from the time series in which more than 500 waves were recorded at the two coasts. In the following analysis, the x-axis is rotated to be the principle direction of incident waves.

Table 1 Statistical characteristics of measured waves

Case No.	Dep. (cm)	r_{10}	r_{01}	r_{11}	r_{12}	r_{21}	γ	U_r	Ku-rt.	Skew.	Q_p
1-1	82	0.806	0.103	-0.004	0.042	0.204	0.305	21.4	3.19	0.162	2.37
1-2	48	0.827	0.101	-0.021	0.148	0.717	0.257	30.7	3.14	0.193	1.84
1-3	97	0.821	0.037	-0.015	0.003	0.412	0.301	6.0	3.27	0.048	2.04
1-4	115	0.819	0.103	-0.020	0.051	0.632	0.392	2.6	2.94	0.023	2.32
1-5	121	0.693	0.161	-0.020	0.019	0.163	0.317	4.6	3.36	0.052	1.90
1-6	134	0.783	0.125	-0.012	0.066	0.680	0.355	4.3	3.07	0.033	1.89
1-7	67	0.596	0.142	-0.022	-0.020	0.656	0.296	24.7	2.71	-0.251	2.72
1-8	113	0.808	0.115	-0.009	-0.291	-0.009	0.299	9.4	2.95	0.016	2.22
2-1	80	0.933	0.026	-0.003	-0.000	0.649	0.307	66.6	3.32	0.144	3.46
2-2	1320	0.906	-0.006	0.000	0.276	0.433	0.431	10.0	2.99	0.107	2.39

Results of Case-number from 1-1 to 1-6 and Case-number from 2-1 to 2-2 correspond to the data obtained at Nishikinohama Beach and Keinomatsubara Beach, respectively. r_{ij} in the table is the covariance defined by Eqs. (11) and (12), γ is the longcrestedness parameter, ν

is the band width parameter and Q_P is the peakedness parameter. Ursell number U_r is calculated by using the significant wave height and the period. The integration of the directional spetrum, which was estimated by EMLM(Isobe et al., 1984), was carried out between $0.5f_p$ and $3f_p$ to obtain m_{12} and m_{21} .

It is found from Table 1 that a large part of measured waves has a significant non-linear property (U_r =2.6-66.6 , Kurtosis=2.939-3.266 , skewness=-0.251-0.193) and had a wide directional spreading(γ=0.2565-0.4306). The value of r_{21} which represents asymmetrical property of directional spreading of incident waves is relatively large when compared with other covariances in the table. However, any correlation between parameters of directional spreading of incident waves (r_{10} and γ) and those of asymmetry of directional spreading(r_{12} and r_{01}) can not be seen.

3.3 Joint Distribution of Wave Height, Period and Direction

In this paper, Case 2-1 whose significant wave height and r_{21} are relatively large and more than 1000 waves were recorded is analyzed as an example to examine the applicability of theoretical joint distribution for H, T and θ derived in this study.

Figure 3 (a)~(c) shows nondimensional scatter diagram of wave period($T/\overline{T}$) and direction(θ) of measured 1000 waves(Case 2-1) under the condition of wave height shown in the figure. The class bands of nondimensional wave heights and directions are 0.25 and 22.5° , respectively. Numerals in the figure show the frequency of zero-down crossing waves. In the figure, predicted isolines of frequency obtained from multiplying the integrated probability density (Eq.(21) between the range of wave height shown in the figure by the total number of measured waves(1000) are also illustrated by solid lines.

Figure 4 is the joint distribution of non-dimensional wave height and directions under the conditions of 0.25< $T/\overline{T}$<0.75 (Fig(a)), 0.75< $T/\overline{T}$<1.25 (Fig(b)) and 1.25< $T/\overline{T}$<1.75 (Fig(c)). Solid lines in the figures are the predicted isolines of frequency calculated in the same way as those in Fig.3.

In Fig. 3, the predicted isolines exhibit almost symmetric profile with respect to the direction when

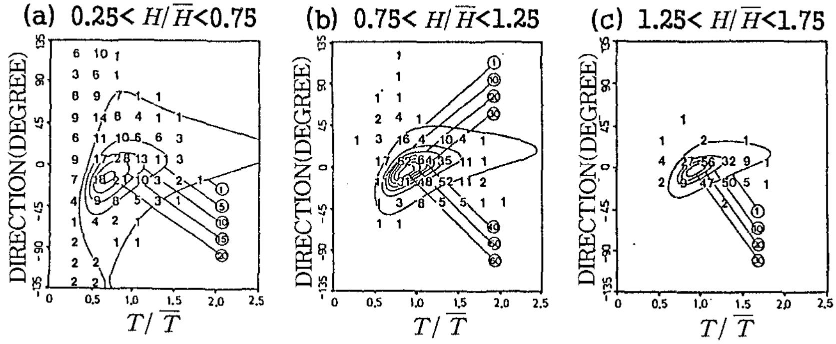

Figure 3 Joint distribution of wave directions and periods

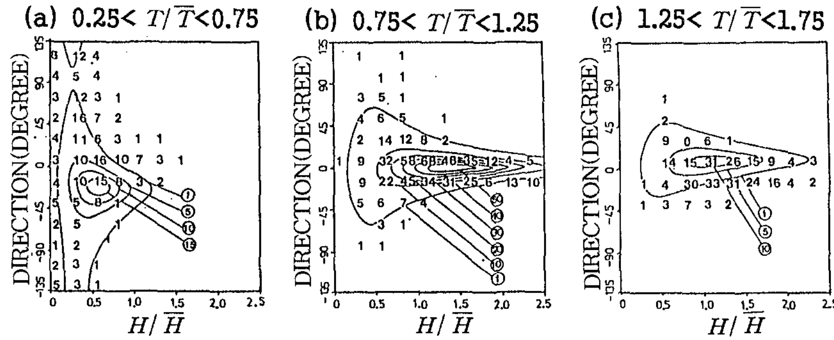

Figure 4 Joint distribution of wave directions and heights

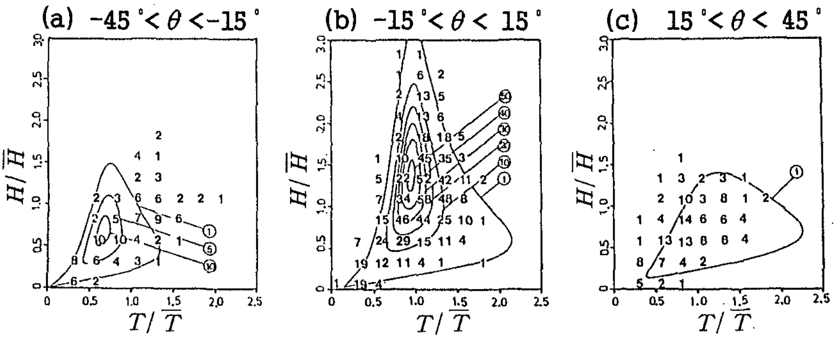

Figure 5 Joint distribution of wave heights and periods

$T/\overline{T}<0.75$. On the other hand, the predicted isolines in Fig.4 show asymmetry around the principle direction ($\theta=0.0°$), ie, wave periods distribute asymmetrically around the principle direction. This difference is partly explained by the fact that wave refraction does not depend deeply on wave heights but mainly on wave periods. It is also found from Figs. 3 and 4 that the predicted isolines do not coincide well with the measured frequency in the region where $T/\overline{T}<0.5$ or $H/\overline{H}<0.5$ or $|\theta|>45°$. However, in the region of $H/\overline{H}>0.75$, $T/\overline{T}>0.75$ and $|\theta|<15°$, where a large part of measured waves is included, a relatively good agreement is seen.

Figure 5 is a scatter diagram of non-dimensional wave heights and periods under the conditions of $-45°<\theta<-15°$ (Fig(a)), $-15°<\theta<15°$ (Fig (b)) and $15°<\theta<45°$ (Fig(c)). Solid lines in the figures are the isolines of frequency calculated in the same way as the former two figures. In the region of $-15°<\theta<15°$, which is shown in Fig.(b), the predicted isolines coincide well with the measured frequency indicating the tail toward the origin in the regions of $T/\overline{T}<0.75$ and $H/\overline{H}<0.75$ due to the correlation between the wave heights and periods. The correlation coefficient between wave heights and periods of Case 2-1 is 0.57.

Although the tail can be seen in Figs.(a) and (c), the agreement between the predicted and measured frequency is not good in these regions. It is also found that the joint distribution of wave heights and periods is not symmetrical with respect to the wave direction by comparing Figs.(a) and (c).

IV. CONCLUSIONS

Summing up the results of the study described above, the followings are the major conclusions:

(1) The joint propability density function of wave height, period and direction is derived by using time series of surface displacement $\eta(t)$, its time derive $\dot{\eta}(t)$, and horizontal two component water particle velocities u(t), v(t) assuming that $\eta(t)$ is a Gaussian process with a narrow band power spectra. It is found that the marginal joint distribution of wave heights and direction has less influence of the asymmetrical property of directional spreading (directional spectra) than that of wave period and direction.

(2) The derived joint distribution are compared with the measured joint distribution in the field of shallow

water. In the region where the appearance frequency of waves is high (ie. $T/\overline{T}>0.75$, $H/\overline{H}>0.75$, $|\theta|<15^{\circ}$) , a relatively high agreement is obtained between measured and predicted frequencies. Especially, the marginal distribution of wave heights and periods in the region of $|\theta|<15^{\circ}$, the predicted frequency coincides fairley well with the measured one. However, in the region of low appearance frequency, both of them do not agree well with each other.

The measured waves had a strong asymmetric property of directional spreading with respect to the principle direction. They also exhibited wide directional spreading and a little nonlinearity.

References

Akai, S., et al., (1988), Joint distribution of wave height, frequency and direction in multi-directional wave fields, Proc. Japanese Conf. on Coastal Engineering, pp. 142~147, in Japanese.

Isobe, M., K. Kondo and K. Horikawa, (1984), Extension of MLM for estimating directional wave spectrum, Proc. Sympo. on Dispersion and Modeling of Directional Seas, Paper No. A-6, 15p.

Isobe, M., (1988), On the joint distribution of wave heights and directions, Proc. 21st Conf. on Coastal Eng., pp. 524~538.

Longuet-Higgins, M. S., (1975), On the joint distribution of the periods and amplitudes of sea waves, Jour. Geophysical Res. Vol. 80, No. 18, pp. 2688~2694.

Mase, H. and Y. Iwagaki, (1982), Wave heights distribution and wave grouping in surf zone, Proc. 18th Conf. on Coastal Eng., pp. 58~76.